FULL PAPER

Dalton
www.rsc.org/dalton

Formation of thallium(I) sandwich M_3TlM_3 clusters, $[(\mu_6\text{-}Tl)M_6(\mu_2\text{-}CO)_6(PEt_3)_6]^+$ (M = Pt, Pd), with two unconnected triangular $M_3(\mu_2\text{-}CO)_3(PEt_3)_3$ units: implications of comparative analysis of isostructural $5d^{10}6s^2$ Tl(I)–$(M_3)_2$ sandwiches (M = Pt, Pd) with known $5d^{10}$ Au(I)–$(Pt_3)_2$ sandwich †

Evgueni G. Mednikov and Lawrence F. Dahl
Department of Chemistry, University of Wisconsin-Madison, Madison, WI 53706, USA. E-mail: dahl@chem.wisc.edu

Received 22nd April 2003, Accepted 11th June 2003
First published as an Advance Article on the web 7th July 2003

The preparation, isolation, and structural/spectroscopic IR, $^{31}P\{^1H\}$ NMR characterization of two new isostructural $5d^{10}6s^2$ Tl(I) sandwich clusters, $[(\mu_6\text{-}Tl)Pt_6(\mu_2\text{-}CO)_6(PEt_3)_6]^+$ (**1**) and $[(\mu_6\text{-}Tl)Pd_6(\mu_2\text{-}CO)_6(PEt_3)_6]^+$ (**2**) as $[PF_6]^-$ salts are presented. Each of these closed-subshell M_3TlM_3 sandwiches (M = d^{10} Pt (**1**), Pd (**2**)) containing two unconnected triangular $M_3(\mu_2\text{-}CO)_3(PR_3)_3$ units is held together solely by delocalized/electrostatic M_3–Tl–M_3 bonding. **1** and **2** were synthesized in *ca.* 90% yields by reactions (under markedly different boundary conditions) of $M_4(\mu_2\text{-}CO)_5(PEt_3)_4$ (M = Pt (**3**), Pd (**4**)) with $TlPF_6$. Their isostructural geometries and stoichiometries were unequivocally established from low-temperature CCD X-ray crystallographic determinations. Both **1** and **2** (without their P-attached ethyl substituents) closely conform to a centrosymmetric trigonal-antiprismatic architecture of trigonal D_{3d} symmetry. A comparison of their well-refined isomorphous crystal structures reveals that the Tl–Pd mean of 2.91 Å in **2** is 0.05 Å smaller than the Tl–Pt mean of 2.96 Å in **1**. In solution, **2** is much more kinetically labile than **1** and (unlike **1**) readily converts under N_2 into the recently reported $[Tl_2Pd_{12}(\mu_2\text{-}CO)_6(\mu_3\text{-}CO)_3(PEt_3)_9]^{2+}$ (**5**) as the $[PF_6]^-$ salt, which was isolated in *ca.* 90% yield from the same reactants (*viz*., $Pd_4(\mu_2\text{-}CO)_5(PEt_3)_4$ and $TlPF_6$). In fact, obtaining crystalline material of **2** from recrystallization procedures was greatly hampered by its facile transformation into large quantities of co-crystallized **5**. A comparative analysis of the molecular parameters and relative stabilities of the closed-subshell $5d^{10}6s^2$ Tl(I)–$(M_3)_2$ sandwiches (M = d^{10} Pt (**1**), Pd (**2**)) with the corresponding known closed-subshell $5d^{10}$ Au(I)–$(Pt_3)_2$ sandwich together with an examination of relative shifts of corresponding bridging carbonyl IR frequencies for selected pairs of related clusters provide compelling evidence that the so-called "inert" $6s^2$ electron-pair on the Tl(I) exerts an overall *destabilizing* influence: namely, that the highly electrophilic $5d^{10}$ Au(I) forms considerably stronger delocalized sandwich Pt_3–Au–Pt_3 bonding (due to its empty, relativistically stabilized 6s acceptor AO) which is presumed to have considerable covalent character. The Tl(I)–Pt(0) distances in **1** are similar to the Tl(I)–Au(I) distances found for another recently reported class of two electronically equivalent closed-subshell Au_3TlAu_3 sandwich units (*i.e.*, $5d^{10}$ Au(I) *vs.* $5d^{10}$ Pt(0)) formed by intercalation of Tl^+ between two electron-rich intramolecular, weakly bonded (aurophilic) Au_3 triangles in trinuclear cyclic gold(I) benzylimidazolate and carbeniate molecules; the Au_3TlAu_3 sandwich units stack into linear chains with intermolecular aurophilic Au(I)–Au(I) interactions between four of the six Au(I) atoms in adjacent units. Of particular interest is that the Tl(I)–Au(I) distances (means, 3.02 and 3.09 Å) in the distorted trigonal-prismatic $(\mu_6\text{-}Tl)Au_6$ sandwich units of the geometrically related Tl^+-intercalated TR(bzim) and TR(carb) complexes are 0.2–0.3 Å longer than the Ag(I)–Au(I) distances (mean, 2.81 Å) in the initially known Au_3AgAu_3 sandwich unit of the Ag^+-intercalated TR(bzim) analogue; it is similarly proposed that this parallel (M′–Au) bond-length difference may likewise be attributed to the considerably smaller electrophilic character of the central $5d^{10}6s^2$ Tl(I) *vs.* that of the $4d^{10}$ Ag(I) due to the overall destabilizing effect of the thallium(I) $6s^2$ electron-pair.

Introduction

The exciting evolution of triangular platinum carbonyl cluster chemistry,[1] pioneered by Chatt and Chini[2] in 1970 on CO/PR_3-ligated Pt_3 triangles and by Chini and Longoni[3] in 1974 on only CO-ligated triangular Pt_3 oligomers, has given rise to the formation of an intriguing bimetallic class of sandwich $Pt_3M'Pt_3$ clusters, $[(\mu_6\text{-}M')Pt_6(\mu_2\text{-}CO)_6L_6]^{n+}$, where two non-linked neutral triangular $Pt_3(\mu_2\text{-}CO)_3L_3$ moieties (L = PR_3) encapsulate a central M′ atom.[4] Such clusters have been reported for closed-subshell electrophilic $d^{10}[M']^{n+}$ metal cations of Groups 11 (Cu(I),[4a] Ag(I),[4b] Au(I);[4a] n = 1) and 12 (Cd(II);[4c] n = 2); crystallographically characterized examples are $[(\mu_6\text{-}Cu)Pt_6(\mu_2\text{-}CO)_6(PPh_3)_6]^+$,[4a] $[(\mu_6\text{-}Ag)Pt_6(\mu_2\text{-}CO)_6(PPr^i_3)_6]^+$,[4b] and $[(\mu_6\text{-}Au)Pt_6(\mu_2\text{-}CO)_6(PPh_3)_6]^+$.[4a] Corresponding bimetallic $[(\mu_3\text{-}M'L)Pt_3(\mu_2\text{-}CO)_3L_3]^+$ clusters (M′ = Cu(I), Ag(I), Au(I); L = PR_3) containing $(\mu_3\text{-}M')Pt_3$ tetrahedra have likewise been prepared and characterized;[5–7] these clusters have previously been denoted[1e] as half-sandwich structures, but herein will be designated as *open-face* sandwiches.[8]

On the other hand, there were no prior reports of any crystallographically characterized examples of corresponding sandwich compounds, $[(\mu_6\text{-}M')Pt_6(\mu_2\text{-}CO)_6L_6]^n$, for the so-called closed-subshell $5d^{10}6s^2$ M′ metals: namely, Tl(I) and Hg(0). Nevertheless, a related zerovalent mercury isocyanide cluster, $(\mu_6\text{-}Hg)Pt_6(\mu_2\text{-}CNR)_6(CNR)_6$ (where R = 2,6-$Me_2C_6H_3$), containing a sandwich Pt_3HgPt_3 core has been synthesized and structurally analyzed.[9] In addition, crystallographic studies

† Dedicated by L. F. D. to John Fackler for his many outstanding professional achievements over the last (nearly) half-century at Case Western Reserve and Texas A & M as a pioneer in transition-metal/gold chemistry and as a highly effective leader in the advancement of modern inorganic chemistry (see, *Inorg. Chem. Award Article*, 2002, **41**, 6959–6972).

DOI: 10.1039/b304409m

established the existences of both the Tl(I)-capping tetrahedral *open-face* sandwich $[(\mu_3\text{-Tl})Pt_3(\mu_2\text{-CO})_3(PCy_3)_3]^+$ as the $[Rh(COD)Cl_2]^-$ salt (with the $5d^{10}6s^2$ Tl(I) weakly interacting with two rhodium-attached chlorine atoms)[7f] and the neutral $[(\mu_6\text{-Hg}_2)Pt_6(\mu_2\text{-CO})_6(PPhPr^i_2)_6]$, which may be considered as two *open-face* $(\mu_3\text{-Hg})Pt_3$ sandwich fragments with the two zero-valent $5d^{10}6s^2$ Hg(0) atoms weakly linked in the solid state.[10a] The mono-mercury sandwich cluster with less bulky PEt_3 ligands, $(\mu_6\text{-Hg})Pt_6(\mu_2\text{-CO})_6(PEt_3)_6$, was prepared by reaction of $Pt_4(CO)_5(PEt_3)_4$ with metallic Hg but was not crystallographically characterized.[10b]

A *hinged* sandwich Pt_3TlPt_3 cluster was reported in 1996 by Puddephatt and coworkers[11a,b] who showed that neutral $Pt_6(\mu_2\text{-CO})_6(\mu_2\text{-dppp})_2(dppp)_2$, which contains two separate triangular $Pt_3(\mu_2\text{-CO})_3(dppp)$ moieties bridged by two μ_2-dppp ligands (where dppp designates the bidentate $Ph_2P(CH_2)_nPPh_2$ group with $n = 3$), functions as a "Venus flytrap" in reacting with $TlPF_6$ to give the *braced* $[(\mu_6\text{-Tl})Pt_6(\mu_2\text{-CO})_6(\mu_2\text{-dppp})_3]^+$ sandwich and free dppp; a crystallographic determination of its $[BPh_4]^-$ salt established that $5d^{10}6s^2$ Tl(I) is encapsulated in a cryptate-like cage consisting of two triangular Pt_3 clusters interconnected by three so-called $(CH_2)_3$ cage bars. They pointed out that the binding of the entrapped Tl(I) triggers the encapsulation process. They also stated that in the absence of the cryptate effect the binding of Tl(I) to Pt_3 clusters would be weak and thereby implied that the existence of the $[(\mu_6\text{-Tl})Pt_6(\mu_2\text{-CO})_6(\mu_2\text{-dppp})_3]^+$ is a consequence of the interconnecting dppp ligands. Puddephatt *et al.*[12] subsequently reported that reaction of $TlPF_6$ with the related *braced* Pt_6 precursor consisting of two Pt_3 moieties interconnected by three mono-methylene chain diphosphines, dppm ($n = 1$), results in an unstable *braced* $[(\mu_3\text{-Tl})_2Pt_6(\mu_2\text{-CO})_6(\mu_2\text{-dppm})_3]^{2+}$ with an external Tl(I) atom capping each of the two Pt_3 triangles due to its cryptate cavity being too small to accommodate a central Tl(I). They also obtained and structurally determined two additional empty *braced* triangular $(Pt_3)_2$ sandwiches containing two external $(\mu_3\text{-Tl})Pt_3$ fragments[12] (*vide infra*).

In striking contrast to platinum, corresponding sandwich clusters of palladium are almost unknown,[1a,e,13] and heretofore examples of sandwich geometries have been limited to only two structurally uncharacterized species: neutral $(\mu_6\text{-Hg})Pd_6(\mu_2\text{-CO})_6(PEt_3)_6$,[14a] whose sandwich formulation was based upon elemental analysis and IR spectroscopy, and $[(\mu_6\text{-Ag})Pd_6(\mu_2\text{-CO})_6(PR_3)_6]^+$, which was only cited in a review[1e] with no literature reference and with no details being given concerning its sandwich formulation including the type of phosphine-attached R substituents. The relative scarcity of triangular palladium carbonyl chemistry[13] may be attributed in large part to the much lower stability of both Pd–Pd and Pd–CO bonding as well as to the much greater kinetic lability of small palladium carbonyl phosphine species; also noteworthy is that no triangular $[Pd_3(\mu_2\text{-CO})_3(PR_3)_3]$ species (as yet) has been unambiguously established by crystallographic characterization.

Herein we present the syntheses and comparative structural analysis of two isostructural sandwich M_3TlM_3 clusters, $[(\mu_6\text{-Tl})M_6(\mu_2\text{-CO})_6(PEt_3)_6]^+$ (M = Pt (**1**), Pd (**2**)), as crystallographically isomorphous $[PF_6]^-$ salts. **1** is the initial example of a sandwich Pt_3TlPt_3 cluster stabilized by only platinum–thallium bonding, while **2** is the first reported example of any crystallographically determined sandwich $Pd_3M'Pd_3$ cluster (where M′ in this case denotes a central closed-subshell d^{10} or $d^{10}s^2$ metal within Groups 11, 12, and 13). This investigation offered the unparalleled opportunity to make a crystallographic comparison of the structures of **1** and **2** in order to determine the geometrical effects resulting from the formal replacement of platinum by palladium atoms within the otherwise identical *triangulo*-$M_3(\mu_2\text{-CO})_3L_3$ units. Of prime significance is a comparative analysis of the molecular architectures and relative stabilities of the corresponding closed-subshell $5d^{10}6s^2$ Tl(I)–$(M_3)_2$ sandwiches (M = Pt (**1**), Pd (**2**)) with the known analogous closed-subshell $5d^{10}$ Au(I)–$(Pt_3)_2$ sandwich, which is given along with an examination of relative shifts of corresponding bridging carbonyl IR frequencies for selected pairs of related clusters.

This work has a direct structural/bonding interrelationship with the closed-subshell Au_3TlAu_3 and Au_3AgAu_3 sandwich units recently determined crystallographically by Burini, Fackler and coworkers[15] from their intercalation of naked $5d^{10}6s^2$ Tl^+ and $4d^{10}$ Ag^+ into stacked chains of trinuclear cyclic gold(I) benzylimidazolate and carbeniate complexes that are luminescent in the solid state (*vide infra*). Furthermore, it has particular relevance to recent experimental/theoretical studies of the structurally unique $Tl_2Pt(CN)_4$ and other Tl–Pt complexes that contain direct $d^{10}s^2$ Tl(I)/d^8 Pt(II) bonding interactions and exhibit intense photoluminescence in crystalline form.[16] Also noteworthy is the recent report[17] describing the synthesis and characterization of crystallographically isomorphous Pd(0) and Pt(0) metallocryptands that encapsulate Tl(I) in a trigonal D_3-symmetric cage to give linear MTlM cores (M = Pd, Pt) for the $[M_2Tl(P_2bpy)_3]^+$ cations (as $[NO_3]^-$ salts); strong metallophilic attractions were proposed[17] from structural analyses that revealed the two identical Tl–Pd and two identical Tl–Pt separations to be 2.77 and 2.80 Å, respectively.

Results and discussion

Stereochemical relationship of sandwich M_3TlM_3 clusters, $[(\mu_6\text{-Tl})M_6(\mu_2\text{-CO})_6(PEt_3)_6]^+$ (M = Pt (1), Pd (2)), and resulting implications

The isostructural geometries of **1** and **2** in their crystallographically isomorphous $[PF_6]^-$ salts are shown in Fig. 1. Although there is no crystallographically imposed site symmetry, both M_3TlM_3 sandwiches in **1** and **2** conform to an idealized trigonal-antiprismatic D_{3d} ($\bar{3}2/m$) geometry, with their twist angles[18] about the three-fold axis from a regular staggered centrosymmetric conformation being 8.0 and 8.7°, respectively, and with their opposite triangular metal planes deviating from co-planarity by 3.4 and 5.2°, respectively. The intertriangular distance between the centroids of the two M_3 triangles of 5.04 Å in **1** and 4.90 Å in **2** conclusively shows the absence of any direct *intertriangular* M_3 bonding interactions.

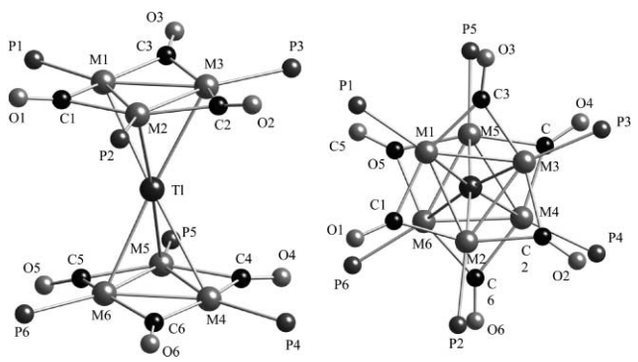

Fig. 1 Side and top views of the virtually identical geometries of the $[(\mu_6\text{-Tl})M_6(\mu_2\text{-CO})_6(PEt_3)_6]^+$ monocations (M = Pt (**1**), Pd (**2**)) with the P-attached Et substituents omitted for clarity. Their isostructural configurations (minus the Et substituents) ideally conform to centrosymmetric trigonal antiprismatic D_{3d} symmetry; no site symmetry within their crystallographically isomorphous $[PF_6]^-$ salts is imposed by the *C*2/*c* space group.

Mean distances and ranges of individual bonding connectivities, which possess unusually small uncertainties that reflect their relatively highly precise crystal-structure determinations, are listed in Table 1. Moreover, Table 1 shows that the individual M–M, M–PEt_3, M–CO(bridging), and C–O bond lengths vary only slightly from their means, whereas the indi-

Table 1 Comparative mean bond lengths under pseudo-D_{3d} trigonal antiprismatic symmetry in $[(\mu_6\text{-Tl})M_6(\mu_2\text{-CO})_6(PEt_3)_6]^+$ clusters, M = Pt (**1**), Pd (**2**), as crystallographically isomorphous $[PF_6]^-$ salts.

		M = Pt (**1**)		M = Pd (**2**)	
Bonding connectivity	N^a	Mean/Å	Range/Å	Mean/Å	Range/Å
Tl–M	6	2.96	2.881(1)–3.127(1)	2.91	2.820(1)–3.119(1)
M–M	6	2.665	2.661(1)–2.670(1)	2.676	2.670(1)–2.687(1)
M–P	6	2.275	2.271(1)–2.279(1)	2.324	2.317(1)–2.334(1)
M–(μ_2-CO)	12	2.075	2.056(5)–2.096(5)	2.082	2.059(3)–2.110(3)
C–O	6	1.170	1.160(7)–1.177(6)	1.154	1.147(4)–1.162(4)

[a] N denotes the number of symmetry-equivalent connectivities under D_{3d} symmetry.

vidual Tl–M distances in both **1** and **2** are markedly irregular; the particular crystallographically related similarities of these observed large dispersions of individual Tl–M connectivities in **1** and **2** may be attributed at least partly to ligand steric effects and crystal packing forces resulting from analogous solid-state orientations within their isomorphous crystal structures.

The salient geometrical difference between **1** and **2** is that the mean Tl–Pd distance of 2.91 Å (range, 2.820(1)–3.119(1) Å) in **2** is 0.05 Å shorter than the mean Tl–Pt distance of 2.96 Å (range, 2.881(1)–3.127(1) Å) in **1**; this smaller Tl–Pd mean was initially surprising in light of the assumption that the much larger relativistic effects of Pt (*vs.* those of Pd) would result in smaller Tl–Pt distances. Especially noteworthy is that the $Pd_3(\mu_2\text{-CO})_3(PEt_3)_3$ triangles in **2** should be significantly less stable than the corresponding Pt_3 ones in **1** due to Pd–Pd and Pd–CO bonding generally being considerably weaker than Pt–Pt and Pt–CO bonding. Furthermore, in solution **2** is much more kinetically labile than **1** and (unlike **1**) readily converts under N_2 into $[Tl_2Pd_{12}(\mu_2\text{-CO})_6(\mu_3\text{-CO})_3(PEt_3)_9]^{2+}$(**5**)[19–21] (*vide infra*).

The Tl–Pt mean of 2.96 Å in **1** is in close agreement with that of 2.93 Å (range, 2.860(3)–2.992 Å) in the previously mentioned *hinged* Pt_3TlPt_3 sandwich of $[(\mu_6\text{-Tl})Pt_6(\mu_2\text{-CO})_6(\mu_2\text{-dppp})_3]^+$.[11a,b] These similar Tl–Pt means suggest that the Tl–Pt bonding interactions are analogous and consequently that the metal-core dimensions within the cryptate-like cage are not significantly influenced by the interconnecting dppp ligands; it is presumed that the steric dimensions (including the bite angle) of the three bridging $Ph_2P(CH_2)_3PPh_2$ ligands instead are accommodated by a low-energy rotational twisting of the two Pt_3 triangles about the pseudo three-fold axis to the observed conformation which is intermediate between the trigonal prism and antiprism. The Tl–Pt mean in **1** is also comparable with those found in three related tetrahedral (*open-face* sandwich) $(\mu_3\text{-Tl})Pt_3$ clusters: namely 3.04 Å in $[(\mu_3\text{-Tl})Pt_3(CO)_3(PCy_3)_3]^+$(isolated as the $[Rh(COD)Cl_2]^-$ salt),[6f] 2.91 Å in $[\{\mu_3\text{-Tl(diketonate)}(OH_2)\}Pt_3(\mu_3\text{-CO})(dppm)_3]^{2+}$,[6g] and 2.90 Å in $[\{\mu_3\text{-Tl(diketonate)}(O_2CCF_3)\}Pt_3(\mu_3\text{-CO})(dppm)_3]^+$.[6g]

The determined Tl–Pd mean of 2.91 Å in **2** is virtually identical to those of 2.89 and 2.92 Å in **5**, both of which have identical Tl/Pd mol ratios. However, these distances are 0.12–0.15 Å longer than the Tl(I)–Pd(0) distance of 2.77 Å in the linear PdTlPd core of D_3 site symmetry in the previously mentioned zerovalent palladium metallocryptand complex.[17]

Table 1 shows that the Pd–Pd mean of 2.676 Å in **2** is only slightly longer than the Pt–Pt mean of 2.665 Å in **1**. Because the corresponding triangular $M_3(\mu_2\text{-CO})_3(PEt_3)_3$ clusters *per se* are not known, a direct comparison of the $5d^{10}6s^2$ Tl(I) coordination effect on M–M distances in M_3 triangles could be made only for $[Pt_3(\mu_2\text{-CO})_3(PCy_3)_3]$;[22] its geometrical capping by Tl^+ to produce the *open-face* $[(\mu_3\text{-Tl})Pt_3(\mu_2\text{-CO})_3(PCy_3)_3]^+$ sandwich[6f] results in a small increase of 0.012 Å in the Pt–Pt mean from 2.655 Å (range, 2.653(2)–2.656(2) Å) to 2.667 Å (range, 2.667(1)–2.668(1) Å).

Comparative analyses of $(\mu_6\text{-M}')M_6$ sandwiches (M = Pt, Pd) and *open-face* $(\mu_3\text{-M}')Pt_3$ sandwiches with closed-subshell $5d^{10}6s^2$ M′ metals (M′ = Tl(I), Hg(0)) *vs.* analogous clusters with electrophilic closed-subshell d^{10} M′ metals (M′ = Cu(I), Ag(I), Au(I)) and resulting implications

(a) Geometrical parameters involving $(\mu_6\text{-M}')M_6$ sandwiches. The observed crystallographically determined variations between the mean Tl–Pt distance in the Pt_3TlPt_3 sandwich of **1** (2.96 Å) and the mean Au–Pt distance in the Pt_3AuPt_3 sandwich of $[(\mu_6\text{-Au})Pt_6(\mu_2\text{-CO})_6(PPh_3)_6]^+$ (2.73 Å) provide compelling geometrical evidence concerning the resulting electronic effect of the central M′ atom on the Pt_3–M′–Pt_3 bond strength: namely, that the much shorter mean Au–Pt distance for the $5d^{10}$ Au(I) *vs.* the mean Tl–Pt distance for the $5d^{10}6s^2$ Tl(I) may be attributed to a significantly *greater* bond strength which would arise from the strong relativistically enhanced acceptor capacity of the empty Au(I) 6s AO (*i.e.*, much larger electrophilic character for Au(I)); in other words, the 0.23 Å-longer mean Tl–Pt distance for the $6s^2$-filled Tl(I) atom may be ascribed to a significantly *smaller* bond strength which would result from the considerably weaker electrophilic acceptor capacity of the higher-energy Tl(I) 6p AO that is not sufficiently counterbalanced by a relatively small nucleophilic donation of its so-called "inert" $6s^2$ electron-pair to the M_3 triangles.

Another major structural variation between sandwiches containing central $5d^{10}6s^2$ M′ atoms (*viz.*, Tl(I), Hg(0)) *vs.* those containing coinage d^{10} M′ atoms (*viz.*, Au(I), Cu(I), Ag(I)) involves the different directional displacements of the six bridging carbonyl ligands from these M_3 planes. Both the symmetrically coordinated doubly bridging carbonyls and triethylphosphine P atoms in **1** and **2** are significantly displaced from their M_3 planes *away from the central* thallium atom with mean deviations of the O, P atoms above the Pt_3 and Pd_3 planes being 0.45, 0.2 Å for **1** and 0.5, 0.2 Å for **2**. Similar out-of-plane CO bending (mean, 0.5 Å) away from the Hg(0) atoms was observed in the two *open-face* $(\mu_3\text{-Hg})Pt_3$ sandwich fragments of the weakly linked zerovalent mercury atoms in $[(\mu_6\text{-Hg}_2)Pt_6(\mu_2\text{-CO})_6(PPhPr^i_2)_6]$.[10a] In contrast, for the crystallographically determined sandwich $Pt_3M'Pt_3$ clusters with $[M']^+$ being either Cu(I), Ag(I), or Au(I) (*vide supra*), each of the P atoms is likewise similarly disposed above the plane (away from the M′ atom) with a mean perpendicular displacement of 0.9 Å, but all bridging CO ligands are bent out-of-plane from their M_3 planes *toward the central* coinage metal atom with mean oxygen deviations of 0.3, 0.8 and 0.3 Å for M′ = Cu(I), Ag(I), and Au(I), respectively.[4a,b] These oppositely directed mean displacements of the bridging CO ligands from their M_3 planes are attributed to different composite electronic/steric effects resulting from the two additional valence s electrons being present in the central isoelectronic Tl(I) and Hg(0) atoms but absent in the coinage M′(I) atoms.

The unchanged directions of displacements of the P-atoms (away from central atoms) are most likely a consequence of the large steric repulsion effects of the P-attached substituents; in

Table 2 Relative shifts of corresponding dominant bridging carbonyl IR frequencies (Nujol) for related pairs of metal carbonyl phosphine clusters.

No. of pair	Related pair[a]	ν(CO)/cm^{-1} for related pair		Shift $\Delta\nu$(CO)/cm^{-1}
1	$Pt_3(CO)_3(PPh_3)_4$[c] / $Pd_3(CO)_3(PPh_3)_4$[d]	Pt_3 / Pd_3	1803, 1788 / 1816	13, 28
2	$Pt_4(CO)_5(PPh_3)_4$[c] / $Pd_4(CO)_5(PPh_3)_4$[d]	Pt_4 / Pd_4	1797 / 1858	61
3	$Pt_4(CO)_5(PEt_3)_4$[e] / $Pd_4(CO)_5(PEt_3)_4$[f]	Pt_4 / Pd_4	1790 / 1844	54
4	$[(\mu_6\text{-Tl})Pt_6(CO)_6(PEt_3)_6]^+$[g] / $[(\mu_6\text{-Tl})Pd_6(CO)_6(PEt_3)_6]^+$[g]	$(\mu_6\text{-Tl})Pt_6$ / $(\mu_6\text{-Tl})Pd_6$	1791 (1806[b]) / 1836 (1856[b])	45 (50)
5	$(\mu_6\text{-Hg})Pd_6(CO)_6(PEt_3)_6$[h] / $[(\mu_6\text{-Tl})Pd_6(CO)_6(PEt_3)_6]^+$[g]	$(\mu_6\text{-Hg})Pd_6$ / $(\mu_6\text{-Tl})Pd_6$	1822 / 1836	14
6	$(\mu_6\text{-Hg})Pt_6(CO)_6(dppp)_3$[i] / $[(\mu_6\text{-Tl})Pt_6(CO)_6(dppp)_3]^+$[i]	$(\mu_6\text{-Hg})Pt_6$ / $(\mu_6\text{-Tl})Pt_6$	1799, 1782 / 1818	19, 36
7	$Pt_4(CO)_5(PEt_3)_4$ / $Pt_4(CO)_5(PPh_3)_4$	PEt_3 / PPh_3	1790 / 1797	7
8	$Pt_4(CO)_5(PEt_3)_4$ / $[(\mu_6\text{-Tl})Pt_6(CO)_6(PEt_3)_6]^+$	Pt_4 / $(\mu_6\text{-Tl})Pt_6$	1790 / 1791	1
9	$[(\mu_6\text{-Tl})Pt_6(CO)_6(PEt_3)_6]^+$ / $[(\mu_6\text{-Au})Pt_6(CO)_6(PPh_3)_6]^+$[j]	$(\mu_6\text{-Tl})Pt_6$ / $(\mu_6\text{-Au})Pt_6$	1791 / 1833	42
10	$[(\mu_6\text{-Tl})Pt_6(CO)_6(PEt_3)_6]^+$ / $[(\mu_6\text{-Cu})Pt_6(CO)_6(PPh_3)_6]^+$[j]	$(\mu_6\text{-Tl})Pt_6$ / $(\mu_6\text{-Cu})Pt_6$	1791 / 1837	46
11	$[(\mu_6\text{-Au})Pt_6(CO)_6(PPh_3)_6]^+$ / $[(\mu_6\text{-Cu})Pt_6(CO)_6(PPh_3)_6]^+$	$(\mu_6\text{-Au})Pt_6$ / $(\mu_6\text{-Cu})Pt_6$	1833 / 1837	4

[a] All cations as $[PF_6]^-$ salts. [b] IR of THF solution. [c] Ref. 2. [d] Ref. 14*d*. [e] Ref. 14*b*. [f] Ref. 14*c*. [g] Present work. [h] Ref. 14*a*. [i] Ref. 11*b*; dppp = $Ph_2P(CH_2)_3PPh_2$. [j] Ref. 4*a*.

fact, the mean perpendicular displacements of the three P atoms from each M_3 plane are *ca.* 0.9 Å in the $[(\mu_6\text{-M}')Pt_6(\mu_2\text{-CO})_6(PPh_3)_6]^+$ sandwiches (M′ = Cu(I), Au(I)) but only *ca.* 0.2 Å in the two $[(\mu_6\text{-Tl})M_6(\mu_2\text{-CO})_6(PEt_3)_6]^+$ sandwiches (M = Pt (**1**), Pd (**2**)). This considerable difference may be attributed mainly to the much larger Tolman cone angle of 145° for the PPh_3 ligands in the Cu(I), Au(I) sandwiches vs. 132° for the PEt_3 ligands[23] in **1**, **2** and to considerable shortening of the two intertriangular M_3 (centroid) distances from 5.04 Å in **1** and 4.90 Å in **2** to 4.27 Å in $[CuPt_6(CO)_6(PPh_3)_6]^+$[4a] and 4.49 Å in $[AuPt_6(CO)_6(PPh_3)_6]^+$.[4a]

(b) Geometrical parameters involving *open-face* (μ_3-M′)M_3 sandwiches. The Tl–Pt means in $[(\mu_3\text{-Tl})Pt_3(\mu_2\text{-CO})_3(PCy_3)_3]^+$ as the $[Rh(COD)Cl_2]^-$ salt (3.04 Å)[6f] and the two other previously mentioned *open-face* $(\mu_3\text{-Tl})Pt_3$ sandwiches (2.91 and 2.90 Å)[6g] and the Hg–Pt mean in the two $(\mu_3\text{-Hg})Pt_3$ tetrahedra of $[(\mu_6\text{-Hg}_2)Pt_6(\mu_2\text{-CO})_6(PPhPr^i_2)_6]$ (2.923–3.084 Å)[10a] are also 0.10–0.25 Å longer than the Au–Pt means in several $[(\mu_3\text{-AuL})Pt_3(\mu_2\text{-CO})_3L_3]^+$*open-face* sandwiches: for example, $[(\mu_3\text{-AuL})Pt_3(\mu_2\text{-CO})_3L_3]^+$(2.75 Å where L = PCy_3),[6a] *hinged* $[(\mu_3\text{-AuPPr}^i_3)_2)Pt_6(\mu_2\text{-CO})_6(\mu_2\text{-dppm})_3]^{2+}$(2.82 and 2.83 Å in two independent dications),[12] and $[(\mu_3\text{-AuL})Pt_3(\mu_2\text{-CO})_2(\mu_2\text{-SO}_2)L_3]^+$(2.76 Å where L = PCy_3).[7d] Noteworthy is that this trend of a 0.25 Å smaller Au–Pt mean in the CO/PCy_3-ligated $(\mu_3\text{-Au})Pt_3$ *open-face* sandwich than the Tl–Pt and Hg–Pt means in the corresponding CO/PCy_3-ligated $(\mu_3\text{-Tl})Pt_3$ analogue and the two *open-face* $(\mu_3\text{-Hg})Pt_3$ sandwich fragments in the previously mentioned CO/$PPhPr^i_2$-ligated $(\mu_6\text{-Hg}_2)Pt_6$ sandwich was initially pointed out by Mingos and coworkers[6f] who stated that "this variation clearly reflects the effect of the filled $6s^2$ shell in the latter two compounds."

(c) Relative stabilities. As mentioned previously, in solution **2** is much more kinetically labile than **1** and readily transforms under N_2 into $[Tl_2Pd_{12}(\mu_2\text{-CO})_6(\mu_3\text{-CO})_3(PEt_3)_9]^{2+}$(**5**). In fact, in solution even **1** is only stable for a few hours under either N_2 or CO. Yamamoto *et al.*[9] found that elimination occurred to give a mercury atom and "free" $Pt_3(\mu_2\text{-CNR})_3(CNR)_3$ when the neutral isocyanide-ligated $[(\mu_6\text{-Hg})Pt_6(\mu_2\text{-CNR})_6(CNR)_6]$ sandwich (R = 2,6-$Me_2C_6H_3$) was heated in toluene at reflux temperature (111 °C). Also noteworthy is that a ^{31}P NMR spectrum (C_6D_6) at –70 °C of the neutral violet–green $[(\mu_6\text{-Hg})Pd_6(\mu_2\text{-CO})_6(PEt_3)_6]$ sandwich exhibited evidence of dynamic behavior likely involving partial dissociation into metallic mercury and $Pd_4(\mu_2\text{-CO})_5(PEt_3)_4$; one of the two observed singlets corresponded to the butterfly precursor, and no ^2J(P,Hg) coupling due to ^{199}Hg (I = 1/2, 16.8%) was observed.[14a] Mingos and coworkers[6f] showed Tl(I) to be sufficiently labile in the *open-face* $[(\mu_3\text{-Tl})Pt_3(\mu_2\text{-CO})_3(PCy_3)_3]^+$ sandwich that the addition of $Au(PCy_3)_3Cl$ led to a quantitative conversion into the known $[(\mu_3\text{-AuPCy}_3)Pt_3(\mu_2\text{-CO})_3(PCy_3)_3]^+$[6a] in which the $[AuPCy_3]^+$ fragment has replaced the Tl^+.

A prime indication that Hg(0) is kinetically more labile than Tl(I) in a *hinged* $Pt_3M'Pt_3$ sandwich is given from the comprehensive studies by Puddephatt and coworkers[11a,b] who reported that the *hinged* sandwich Pt_3TlPt_3 cluster, $[(\mu_6\text{-Tl})Pt_6(\mu_2\text{-CO})_6(\mu_2\text{-dppp})_3]^+$ is slowly formed along with some decomposition by replacement of Hg(0) in the corresponding *hinged* sandwich Pt_3HgPt_3 analogue $[(\mu_6\text{-Hg})Pt_6(\mu_2\text{-CO})_6(\mu_2\text{-dppp})_3]$ with Tl^+ from the reaction with $TlPF_6$. They observed that this reaction is accelerated in the presence of "free" dppp. They proposed that direct loss of mercury from the *braced* analogue is impossible and that opening up of one of the μ_2-dppp bridges (aided by "free" dppp) must occur prior to the Tl^+-for-Hg(0) metal exchange.

In sharp contrast, similarly ligated $Pt_3M'Pt_3$ sandwiches or *open-face* $(\mu_3\text{-M}'PR_3)Pt_3$ sandwiches containing electrophilic coinage d^{10} $[M']^+$ metals (M′ = Cu(I), Ag(I), Au(I)) are generally more air-stable in the solid state.

(d) Corresponding dominant carbonyl IR frequencies for related pairs of metal clusters. A direct comparison of the relative shifts of the corresponding dominant bridging carbonyl IR frequencies for 11 pairs of closely related metal carbonyl clusters presented in Table 2 is highly informative concerning an evaluation of the relative donor/acceptor capacity (*i.e.*, nucleophilic/electrophilic character) of both the central M′ atom and two M_3 triangles in the $M_3M'M_3$ sandwiches presented herein. The first three entries in Table 2 reveal that the CO frequencies for the three platinum clusters are considerably lower than the corresponding ones for the *identically ligated* palladium clusters; these relative CO-frequency differences are consistent with d_π(M)–π*(CO) backbonding generally being considerably greater for M = Pt than for M = Pd, which points to the negative charge density being larger on the carbonyl ligands and smaller on the Pt atoms. The CO-frequency shift in the fourth entry likewise is in accordance with the first three entries in suggesting for the *identically ligated* $(\mu_6\text{-Tl})M_6$ cores (M = Pt, Pd) the occurrence of considerably greater d_π(M)–π*(CO) backbonding for M = Pt.

Entries **5** and **6** compare the CO-frequency shifts for *non-hinged* and *hinged* $(\mu_6\text{-Hg})M_6$ sandwiches *vs. identically ligated* analogous $(\mu_6\text{-Tl})M_6$ sandwiches for M = Pd and Pt, respectively. These entries reveal lower CO frequences for both the *non-hinged* and *hinged* Hg(0) sandwiches relative to those for the corresponding two Tl(I) sandwiches. This suggests that $5d^{10}6s^2$ Hg(0) is a better nucleophile (less electrophilic) than $5d^{10}6s^2$ Tl(I) in donating its $6s^2$ electron-pair (*i.e.*, Hg(0) is a better *net* charge donor and Tl(I) a better *net* charge acceptor); a larger negative charge density on the M_3 triangles should result for each Hg(0) sandwich, which in turn would give rise to better d_π(M)–π*(CO) backbonding for both Hg(0) sandwiches. This same conclusion was previously stated by Puddephatt and coworkers[11] from an IR analysis of their *hinged* hexaplatinum sandwiches of Tl(I) and Hg(0).

Entry 7 indicates only a small CO-frequency shift in the butterfly Pt_4 clusters upon formal substitution of PEt_3 ligands for PPh_3 ones. Entry 8 indicates that the change from the triethylphosphine Pt_4 butterfly geometry to the triethylphosphine $(\mu_6\text{-Tl})Pt_6$ sandwich geometry also gives rise to a negligible CO-frequency shift. These two entries are consistent with the premise that ν(CO) shifts due to different PEt_3 and PPh_3 ligands can be ignored in a comparison of the sandwich $(\mu_6\text{-M}')Pt_6$ clusters given in entries 9 and 10. Entries 3 and 4 likewise reveal for the related palladium pair, $Pd_4(CO)_5(PEt_3)_4$/$[(\mu_6\text{-Tl})Pd_6(CO)_6(PEt_3)_6]^+$, that the analogous ν(CO) shift is also small.

Entries 9, 10 and 11 involve a comparison of CO-frequency shifts for $(\mu_6\text{-M}')Pt_6$ sandwiches with M′ = Tl(I) *vs.* M′ = Au(I) and Cu(I). Entries 9 and 10 are of particular importance in providing convincing evidence that $5d^{10}$ Au(I) and $3d^{10}$ Cu(I) are highly electrophilic compared to $5d^{10}6s^2$ Tl(I) in removing negative charge from the Pt_3 triangles such that the d_π(Pt)–π*(CO) backbonding is markedly decreased in each case.

Entry 11 suggests that the electrophilicities of Au(I) and Cu(I) in $Pt_3M'Pt_3$ sandwiches are similar. A previous comparative IR analysis by Puddephatt and coworkers[12] of their *braced* $[(\mu_3\text{-M}'PPh_3)_2Pt_6(\mu_2\text{-CO})_6(\mu_2\text{-dppm})_3]^{2+}$ clusters with two external μ_3-$[M'PPh_3]^+$ fragments (for M′ = Cu(I), Ag(I), Au(I)) as $[PF_6]^-$ salts relative to the neutral *hinged* $[Pt_6(\mu_2\text{-CO})_6(\mu_2\text{-dppm})_3]$ revealed CO-frequency shifts consistent with diminished d_π(Pt)–π*(CO) backbonding that indicated the relative electrophilicities for the μ_3-$[M'PPh_3]^+$ fragments to be Cu > Au > Ag.

Also of prime interest is an examination of the electronic effect on the $\Delta\nu$(CO) shift that arises in an *identically ligated open-face* $(\mu_3\text{-M}')Pt_3$ sandwich due to the formal replacement of Tl(I) by a *phosphine-attached* Au(I). Such a replacement was actually shown to occur when $[(\mu_3\text{-Tl})Pt_3(\mu_2\text{-CO})_3L_3]^+$ as the $[PF_6]^-$ salt (where L = PCy_3) [ν(CO) = 1864 (s), 1798 (m) cm^{-1}, Nujol][6f] was transformed quantitatively by reaction with AuLCl into $[(\mu_3\text{-AuL})Pt_3(\mu_2\text{-CO})_3L_3]^+$ as the $[PF_6]^-$ salt (L = PCy_3) [ν(CO) = 1805 cm^{-1}, Nujol].[6a] A comparison of their corresponding *dominant* CO-frequencies with that of 1770 cm^{-1}(Nujol) for the neutral triangular $Pt_3(\mu_2\text{-CO})_3(PCy_3)_3$[22,24] indicates that the electrophilic character of Au(I) has decreased so much *via* its attachment to the electron-donating PCy_3 ligand that $(\mu_3\text{-Tl})^+$ (with $\Delta\nu$(CO) = 94 cm^{-1}) is now a better electrophile than the μ_3-$[AuPCy_3]^+$ fragment (with $\Delta\nu$(CO) = 35 cm^{-1}) relative to neutral $Pt_3(\mu_2\text{-CO})_3(PCy_3)_3$.[25–27]

Gradient-corrected (scalar-relativistic) DFT calculations have been carried out on PH_3-models of **1** and **2** and on sandwich models, $[(\mu_6\text{-M}')M_6(\mu_2\text{-CO})_6(PH_3)_6]$ (M′ = Au^+, Hg, Tl^+; M = Pd, Pt) together with corresponding *open-face* (tetrahedral) $[(\mu_3\text{-M}')M_3(CO)_3(PR_3)_3]$ sandwich models (M′ = Au^+, Hg, Tl^+; M = Pd, Pt; R = H, Me); resulting geometrical/electronic consequences will be given elsewhere.[28]

Comparative analysis of closed-subshell $M_3M'M_3$ sandwiches in $[(\mu_6\text{-M}')M_6(\mu_2\text{-CO})_6(PR_3)_6]^+$ clusters (M′ = Tl(I), Au(I), Ag(I); M = Pd(0), Pt(0)) with known closed-subshell $Au_3M'Au_3$ sandwich units in M'^+ -intercalated trinuclear cyclic gold(I) benzylimidazolate and carbeniate complexes (M′ = Tl(I), Ag(I)) and resulting implications

Two electronically equivalent trigonal-prismatic closed-subshell Au_3TlAu_3 sandwich units (*i.e.*, d^{10} Au(I) *vs.* d^{10} Pt(0)) formed by the intercalation of Tl^+ into structurally similar trinuclear cyclic gold(I) complexes of benzylimidazolate (denoted as TR(bzim) and carbeniate (denoted as TR(carb) were recently reported by Burini, Fackler and coworkers.[15b,c] These and the previously characterized Ag^+-intercalated TR(bzim) analogue[15] consist of naked $5d^{10}6s^2$ Tl^+ or $4d^{10}$ Ag^+ ions centered between two weakly bonding (aurophilic) Au_3 units, each formally constructed by the linkage of three linear C–Au(I)–N fragments into a nearly planar nine-membered ring in the geometrically related TR(bzim) and TR(carb)) complexes. For each of these three compounds extended linear chains are produced by intermolecular aurophilic Au–Au interactions (range, 3.05–3.26 Å), in which four of the six Au(I) atoms of a given $Au_3M'Au_3$ sandwich interact with two Au(I) atoms on each of the two neighboring clusters. Resulting Tl(I)–Au(I) distances in the TR(bzim) complex (mean, 3.02 Å; range, 2.971(1)–3.045(1) Å)[15b,c] and TR(carb) complex (mean, 3.09 Å; range, 3.067(1)–3.108(1) Å are similar to those in **1**, whereas the Ag(I)–Au(I) distances in the TR(bzim) complex (mean, 2.81 Å; range, 2.731(2)–2.922 Å)[15] are 0.2–0.3 Å shorter.[28] Particularly noteworthy is that this considerable difference between the M′–Au distances within the $Au_3M'Au_3$ sandwich units for the two $5d^{10}6s^2$ Tl(I) sandwiches compared to the $4d^{10}$ Ag(I) sandwich unit parallels the corresponding 0.2 Å -longer Tl–Pt distances within the electronically equivalent $Pt_3M'Pt_3$ sandwich for $5d^{10}6s^2$ Tl(I) in **1** compared to the $5d^{10}$ Au(I) in $[(\mu_6\text{-Au})Pt_6(\mu_2\text{-CO})_6(PPh_3)_6]^+$.[4a] On this basis, we propose that this (M′–Au) bond-length difference within the $Au_3M'Au_3$ sandwich units may likewise be a consequence of the considerably smaller electrophilic character of the central $5d^{10}6s^2$ Tl(I) *vs.* that of the $4d^{10}$ Ag(I) on account of the overall destabilizing effect of the thallium(I) $6s^2$ electron-pair.[29]

Synthesis and relative reactivities of 1 and 2

Both **1** and **2** were prepared in high yields (*ca.* 90%) from corresponding stoichiometric reactions of $TlPF_6$ with analogous neutral butterfly-shaped tetrametallic $M_4(\mu_2\text{-CO})_5(PEt_3)_4$ (M = Pt (**3**),[14b] Pd (**4**)[14c]) precursors but were obtained under markedly different experimental reaction conditions (*vide infra*).

$$3\,M_4(\mu_2\text{-CO})_5(PEt_3)_4 + 2\,TlPF_6 \longrightarrow 2[(\mu_6\text{-Tl})M_6(\mu_2\text{-CO})_6(PEt_3)_6][PF_6] + 3\,CO \quad (1)$$

1 was also synthesized in a much smaller yield (*ca.* 35%) from $Pt_5(CO)_6(PEt_3)_4$[30] as starting material instead of **3**; the precursor $Pt_5(CO)_6(PEt_3)_4$ was obtained from a different preparative route[14b] than that originally reported.[30] In complete contrast to **1** which is relatively stable in solution under N_2, **2** is unstable and readily converts into $[Tl_2Pd_{12}(\mu_2\text{-CO})_6(\mu_3\text{-CO})_3(PEt_3)_9]^{2+}$(**5**);[19–21] therefore, **2** was synthesized under reaction conditions that involved its immediate precipitation into the solid state. The spontaneous conversion of **2** into **5**, which was revealed in this research, played a crucial role in ascertaining its metal-core identity as Tl_2Pd_{12}.[19] This reaction occurs more readily *via* assistance of O_2 (air):

$$2[(\mu_6\text{-Tl})Pd_6(CO)_6L_6]^+ + [(3+x)/2]\,O_2 \longrightarrow [Tl_2Pd_{12}(CO)_9L_9]^{2+} + 3\,OL + x\,CO_2 + y\,CO \quad (2)$$

where L = PEt_3 and $x + y = 3$; the transformation of **2** into **5** is readily detected by a color change from the dichroic deep blue–red of **2** to the red–brown of **5**. Its reaction stoichiometry is still unclear, even though the intermediate formation of **2** in the reaction of **4** with $TlPF_6$ under N_2 is clear-cut. **2** was converted into **5** by two ways: (a) *via* the generation of **2** *in situ* from the reaction of **4** with $TlPF_6$; and (b) *via* the direct conversion of a fine crystalline sample of **2** in solution.

Difficulties were encountered in obtaining suitable single crystals of **2** for X-ray diffraction studies, because in general crystal-growing from solution is a relatively slow process, whereas solutions of **2** are unstable either under inert atmosphere (*e.g.*, N_2, Ar due to rapid transformation into **5**) or under CO. Fortunately, this challenge was overcome, and single crystals of **2** were prepared in small quantities and separated mechanically *via* the Pasteur technique[31] from the co-crystallized mixture primarily composed of crystalline **5**. Particularly

noteworthy is that crystals of **2** were recognized from otherwise analogous large black crystals of **5** on the basis of their opalescent nature (see Experimental section).

Spectroscopic characterization of 1, 2 and resulting implications

IR spectra. These spectra showed that the bridging COs in **1** are lower by 45 cm^{-1} (Nujol) and 50 cm^{-1} (THF) than corresponding ones in **2**. As presented earlier, these relatively large CO-frequency variations are in accordance with the occurrence of considerably less $d_{\pi}(M)$–$\pi^*(CO)$ backbonding in **2** (M = Pd) than that in **1** (M = Pt); this same IR trend is observed in a previous comparison of identically ligated neutral trinuclear and tetranuclear carbonyl/phosphine clusters of platinum and palladium, (Table 2, pairs 1–3).

Presumed non-rigidity of solid-state $[(\mu_6\text{-Tl})M_6(\mu_2\text{-CO})_6(PEt_3)_6]^+$ sandwiches (M = Pt (1), Pd (2)) in solution

(a) General comments. A particularly intriguing structural aspect of small platinum carbonyl/phosphine clusters and the triangular $[Pt_3(CO)_6]_n^{2-}$ oligomers (n = 1, 2, 3) is their indicated stereochemical non-rigidity in solution based upon multinuclear NMR measurements.[3c,32,33] One striking illustration is given by the $Pt_4(CO)_5(PR_3)_4$ clusters (R = Me_2Ph,[32a,34a] Et [34b]) which have a solid-state butterfly geometry of four Pt atoms with five CO-bridging bonding edges and one non-bonding edge; both $^{31}P\{^1H\}$ and ^{195}Pt NMR solution spectra revealed magnetically equivalent platinum and phosphorus atoms which were interpreted *via* a dynamic tetrahedral model to involve a time-averaging of all possible isomeric edge-opened (butterfly) Pt_4 tetrahedra along with rapid scrambling of the CO ligands.[32] Another classic example is the solid-state trigonal-prismatic stacking [3a] of three $[Pt_3(\mu_2\text{-CO})_3(CO)_3]$ units in $[Pt_9(CO)_{18}]^{2-}$, for which an analysis [3c,33] of its ^{195}Pt NMR solution spectrum provided a dynamic model involving rapid rotation of the two outer Pt_3 triangles with respect to the middle Pt_3 triangle about the principal three-fold axis.

(b) Room-temperature $^{31}P\{^1H\}$ NMR solution spectra of 1 and resulting implications. For metal nuclei of **1** there are two NMR-active thallium nuclei (I = 1/2 for ^{203}Tl, 29.5%; I = 1/2 for ^{205}Tl, 70.5%) and one NMR-active platinum nucleus (I = 1/2 for ^{195}Pt, 33.8%). $^{31}P\{^1H\}$ and ^{195}Pt NMR studies of $Pt_3(CO)_3(PR_3)_3$ clusters were reported by Moor, Pregosin and Venanzi [24] for PCy_3, PPr^i_3, PPr^i_2Ph, and $P(CH_2Ph)Ph_2$. Both $^{31}P\{^1H\}$ and ^{195}Pt spectra of $Pt_3(CO)_3(PR_3)_3$ were modeled under pseudo-D_{3h} symmetry as the combination of four triangular isotopomers of 0, 1, 2, 3 ^{195}Pt nuclei with the following abundance and spin-system for each isotopomer (where A = ^{31}P, X = ^{195}Pt): 0 (29.63%, A^3), 1 (44.44%, AA'_2X), 2 (22.22%, $AA'A''XX'$), 3 (3.7%, $AA'A''XX'X''$). The low natural abundance and spectral complexity of the fourth isotopomer with 3 ^{195}Pt nuclei precluded its consideration in interpretations of the $^{31}P\{^1H\}$ and ^{195}Pt spectra. Their analysis for the room-temperature solution $^{31}P\{^1H\}$ spectra of the four different phosphines provided simulated spectra with coupling constants in good agreement with measured values.

For **1** in solution it is presumed that a dynamic process involving rapid rotations of platinum triangles about the three-fold axis through Tl(I) is most likely. Its $^{31}P\{^1H\}$ NMR spectrum (acetone-d_6) under N_2 atmosphere has a broadened doublet pattern composed of two singlet patterns of $Pt_3(CO)_3(PR_3)_3$ [1b,24] due to the ^{203}Tl,^{205}Tl coupling. This ^2J(P,Tl) coupling clearly indicates a retention of the sandwich Pt_3TlPt_3 structure in solution. The observation in the $^{31}P\{^1H\}$ NMR spectrum of **1** of only the doublet pattern of the spectrum of $Pt_3(CO)_3(PR_3)_3$ additionally indicates a rapid rotation of platinum triangles; otherwise, the character of this spectrum would be expectedly more complicated due to additional diverse combinations of platinum isotopomers for the observed static (solid-state) structure of **1** being retained in solution. All observed coupling constants in **1** are within ranges (given in parentheses) that are typical for $Pt_3(CO)_3(PR_3)_3$: namely, ^1J(P,Pt), 4450 Hz (range, 4412–4751 Hz); ^2J(P,Pt), 444 Hz (range, 413–488 Hz); ^3J(P,P), 49 Hz (range, 49–63 Hz).[24]

Interactions between Tl(I) and the Pt_3 triangles in **1** can be readily affected by addition of a small quantity of "free" Tl^+: namely, mol ratio $(\mu_6\text{-Tl})Pt_6/Tl^+$ = 1/0.1); a $^{31}P\{^1H\}$ NMR spectrum then showed no evidence of ^2J(P,Tl) coupling and instead of doublet signals exhibited single signals, typical for that of $Pt_3(CO)_3(PR_3)_3$ [24] that were broader than those obtained for **1**. This effect indicates a fast exchange process between $Pt_3(CO)_3(PEt_3)_3$ triangles and Tl(I), which is initiated by the added "free" Tl^+ ions.

(c) Room-temperature $^{31}P\{^1H\}$ NMR solution spectra of 2 and resulting implications. *(1) Spectra under CO atmosphere.* An analogous dynamic process involving rapid rotations of Pd_3 triangles was initially presumed to occur for **2** in solution. However, a $^{31}P\{^1H\}$ NMR spectrum (acetone-d_6) of **2** under CO displayed a strong broad asymmetric signal at 24.2 ppm with a broad but distinguishable shoulder at ~21.5 ppm. After 21 days of storage in an NMR tube at room temperature under CO, a repeated spectrum did not reveal any significant changes. In spite of this observation, we were unsuccessful in growing single crystals of **2** under CO; instead, slow decomposition occurred.

In contrast to the observed spectrum of **2** in acetone-d_6 solution under CO, a $^{31}P\{^1H\}$ NMR spectrum of **2** in the more polar acetonitrile-d_3 solution under CO displayed, in addition to the asymmetric broad signal of **2**, six of the ten distinguishable signals [19] characteristic of $[Tl_2Pd_{12}(CO)_9(PEt_3)_9]^{2+}$ (**5**). Both solution spectra of **2** displayed a weak unassigned signal at 16.0 ppm (acetone-d_6) and 16.4 ppm (acetonitrile-d_3).

(2) Spectra under N_2 atmosphere. $^{31}P\{^1H\}$ NMR spectra of **2** under N_2 were found to undergo significant changes with time; ~15 min after dissolution of **2** in acetone-d_6, two strong broad overlapping signals at 23.3 and ~21.0 ppm with approximately equal intensities were observed together with 9 of the 10 well-defined signals previously found for $[Tl_2Pd_{12}(CO)_9(PEt_3)_9]^{2+}$ (**5**).[19] Six of these signals (from 26.3 to 21.3 ppm) overlapped with the broad signals of **2** but were readily distinguishable due to their much narrower widths. After 3 h the two broad signals of **2** merged to give a broad singlet at ~22.0 ppm, while relative intensities of the signals due to **5** increased only slightly.[35] Both spectra contained an unassigned weak signal at 6.0 ppm.

Noteworthy is that $^{31}P\{^1H\}$ NMR spectra of **2** in acetone-d_6 solution under N_2 (in contradistinction with analogous spectra under CO) clearly demonstrated the occurrence of a conversion of **2** into **5**. A different time-dependent behavior of **2** in forming **5** was expectedly found from similar spectra of **2** in acetonitrile-d_3 solution under N_2.

In addition to complications caused by conversion of **2** to **5**, $^{31}P\{^1H\}$ NMR spectra of **2** at room temperature strongly suggest the occurrence of more complex dynamic processes in solution than in case of **1**. This process may include dissociation-reassociation of **2** with formation of "free" $Pd_3(CO)_3(PEt_3)_3$ triangles and their further transformations. In the case of a non-rigid process involving only *rapid* rotations of triangles, $^{31}P\{^1H\}$ NMR solution spectra of **2** would be expected to have a simple doublet (due to the ^2J(P,Tl) coupling) for equivalent P atoms with sufficiently narrow signals closely related to corresponding ones in $^{31}P\{^1H\}$ NMR spectra of **1** arising from the particular isotopomer with all non-magnetic platinum nuclei. However, the observed spectra of **2** had either a complex asymmetric broad signal (under CO atmosphere) or an approximately symmetrical broad pattern that dramatically changed with time (under N_2 atmosphere). In both cases the

half-width at half-height of these extremely broadened signals of **2** were ~10 times larger than those of **1**.

Future work includes carrying out multinuclear NMR measurements of **1** and **2** at room and low-temperature in order to obtain more detailed structural information on these clusters in solution together with an investigation of the reactivities of **1** and **2** with Group 11 metals. Recently we isolated and characterized an intriguing Tl_4Pd_{22} cluster from direct reaction of **2** with $Au(SMe_2)Cl$.[36]

Experimental

Materials and methods

Reactions and manipulations were carried out *via* standard Schlenk techniques on a preparative vacuum line under nitrogen atmosphere. All solvents were dried and distilled under nitrogen immediately prior to use. The following drying agents were used: THF (K/benzophenone), acetone ($CaCO_3$), and acetonitrile (Na_2CO_3). $Pd_4(CO)_5(PEt_3)_4$ was prepared from a literature synthesis;[14c] likewise, $Pt_4(CO)_5(PEt_3)_4$ and $Pt_5(CO)_6(PEt_3)_4$ were synthesized as previously described.[14b] Other chemicals were purchased and used without further purification.

$^{31}P\{^1H\}$ NMR spectra were obtained on a Bruker AM-300 spectrometer and referenced to 85% H_3PO_4 in D_2O as an external standard. Each NMR sample was prepared *via* a pump–thaw technique. Infrared spectra were recorded on a Mattson Polaris FT-IR spectrometer by use of a nitrogen-purged CaF_2 cell.

All yields were calculated on the basis of Pt or Pd metals.

Synthesis and spectroscopic characterization of $[(\mu_6\text{-Tl})Pt_6(\mu_2\text{-CO})_6(PEt_3)_6]^+$, 1, and $[(\mu_6\text{-Tl})Pd_6(\mu_2\text{-CO})_6(PEt_3)_6]^+$, 2, as $[PF_6]^-$ salts

(a) $[(\mu_6\text{-Tl})Pt_6(\mu_2\text{-CO})_6(PEt_3)_6][PF_6]$. In a typical reaction, a solution of $TlPF_6$ (0.102 g; 0.292 mmol) in 10 mL of THF was added under Ar atmosphere to a stirred solution of $Pt_4(CO)_5(PEt_3)_4$ (**3**) (0.608 g; 0.436 mmol) in 5 mL of THF; an immediate reaction occurred with formation of a dichroic green (reflection)/red (transmission) solution. After being stirred for 2 h, 2 mL of heptane were added; slow evaporation of the solvent to a final volume of ~4 mL gave rise to the formation of 0.632 g of a crystalline black–violet precipitate of $[(\mu_6\text{-Tl})Pt_6(\mu_2\text{-CO})_6(PEt_3)_6]^+$ (**1**) as the $[PF_6]^-$ salt (91% yield). IR spectra exhibited bridging carbonyl bands in Nujol at 1852 (m), 1809 (sh), 1791 (s) cm^{-1} and in THF solution at 1857 (m), 1806 (vs), 1776 (w) cm^{-1}. $^{31}P\{^1H\}$ NMR spectrum (121 MHz, acetone-d_6, N_2 atmosphere): δ 53.5 ppm (d, $^1J(P,Pt)$ = 4450 Hz, $^2J(P,Tl)$ = 445 Hz, $^2J(P,Pt)$ = 444 Hz, $^3J(P,P)$ = 49 Hz), −139.8 ppm (septet, $^1J(P,F)$ = 707 Hz).

Single crystals of **1** were obtained by slow diffusion of hexane into THF solution, and one with size of 0.42 × 0.26 × 0.18 mm^3 was used for X-ray data collection.

(b) $[(\mu_6\text{-Tl})Pd_6(\mu_2\text{-CO})_6(PEt_3)_6][PF_6]$. Unlike the preparation of **1**, the synthesis of $[(\mu_6\text{-Tl})Pd_6(\mu_2\text{-CO})_6(PEt_3)_6]^+$ (**2**) as the $[PF_6]^-$ salt necessitated: (a) the presence of a CO atmosphere; and (b) immediate isolation of **2** in the solid state. This was achieved by the fast addition of a solution of $Pd_4(CO)_5(PEt_3)_4$ (**4**) (*e.g.*, 0.322 g; 0.310 mmol) in 10 mL of hexane to a solution of $TlPF_6$ (0.072 g; 0.206 mmol) in a minimal amount of THF (3 mL) under vigorous stirring. **2** was immediately formed and isolated as dark violet fine crystalline powder (0.340 g; 88% yield). IR spectra displayed the same three-band pattern of bridging carbonyl frequencies (as found for **1**) in Nujol at 1891 (m), 1859 (sh), 1836 (s) cm^{-1} and in THF solution at 1897 (m), 1856 (vs), 1825 (w) cm^{-1}. $^{31}P\{^1H\}$ NMR spectrum (121 MHz, acetone-d_6, CO atmosphere): δ 24.2 (br), ~21.5 (br), 16.0 (w), −139.8 ppm (septet, $^1J(P,F)$ = 708 Hz); (acetonitrile-d_3, CO atmosphere): δ 30.4, 28.9, 28.5, 26.4, 22.4, 21.7 (all are weak signals of **5**), 22.7 (br), 16.4 (w), −140.1 ppm (septet, $^1J(P,F)$ = 706 Hz); (acetone-d_6, N_2 atmosphere): 30.2, 28.7, 28.5, 26.3, 25.5, 24.6, 22.3, 21.6, 21.3 (all are signals of **5**), 23.3 (br), ~21.0 (br), 6.0 (br w) –139.8 ppm (septet, $^1J(P,F)$ = 712 Hz).

(c) Conversion of 2 into $[Tl_2Pd_{12}(CO)_9(PEt_3)_9]^{2+}$, 5, and preparation of single crystals of 2. A mixture of $Pd_4(CO)_5(PEt_3)_4$, **4**, (0.278 g; 0.268 mmol) and $TlPF_6$ (0.062 g; 0.177 mmol) (molar ratio 3/2) was dissolved in 6 mL THF under N_2. The resulting dichroic blue/red solution of **2**, which was instantly formed *in situ*, was immediately set up for crystallization *via* hexane vapor diffusion in a small "free" volume (~20 mL) flask in order to maintain a suitable *self-residual* pressure of CO. After ten days 0.250 g (85% yield) of large black crystals of $[Tl_2Pd_{12}(CO)_9(PEt_3)_9]^{2+}$ **5** as the $[PF_6]^-$ salt and 0.012 g (4% yield) of large black opalescent crystals (green after crushing) of **2** were separated under a microscope. About 2 mg of crystals consisted of joined blocks of crystalline **2** and **5**. A cut crystal of size 0.30 × 0.22 × 0.20 mm^3 was used for X-ray data collection of **2**. Crystals of the $[PF_6]^-$ salt of **5** were identified spectroscopically and from a single-crystal X-ray diffraction examination. The formation of small amounts of crystalline **2** in this procedure could be easily avoided just by changing the atmosphere during the first few hours of reaction.

Subsequent direct reactions showed that **2** (0.08–0.15 g), which was prepared in the form of fine dark violet crystalline powder (as described above) and then dissolved in 10–20 mL of THF, acetone, or acetonitrile under a gentle stream of N_2 gas in order to remove emitted CO, converted to **5** as well. During these reactions the color of solution gradually changed (over 0.5 ÷ 3 h) from the initial dichroic blue–red color of **2** to the red–brown color of **5**, whose identity was ascertained spectroscopically. Qualitatively the rates of conversion of **2** into **5** were found to increase upon changes in solvent polarity with THF < acetone < acetonitrile. The addition of O_2 (air) was observed to greatly facilitate the rate of transformation of **2** into **5** as the main product (*i.e.*, the reaction being completed within 20–60s) presumably by the oxidative deligation from **2** of PEt_3 and of some of the CO ligands which form triethylphosphine oxide and CO_2 byproducts, respectively (see eqn. (2)). Furthermore, **2** was found to convert into **5** as the main product (which was extracted, crystallized, and then spectroscopically/crystallographically identified) even in the solid state at room temperature after 3–4 weeks of storage under Ar. It was observed that **2** could be preserved for at least two weeks in the solid state only under CO atmosphere.

X-Ray crystallographic analyses

General procedures. X-Ray data for the isomorphous crystals of [**1**][PF_6] and [**2**][PF_6] were collected at 100(2) K *via* a Bruker SMART CCD-1000 area detector diffractometer with graphite-monochromated Mo-Kα radiation (λ = 0.71073 Å) from a sealed-tube generator. The crystal structure of [**1**][PF_6] was determined from direct methods, and the resulting coordinates for the non-hydrogen atoms obtained from least-squares refinement were then used as initial atomic coordinates for the corresponding atoms in [**2**][PF_6]. Least-squares refinements (based on F^2) were carried out with SHELXTL.[37]

CCDC reference numbers 202091 and 202092.

See http://www.rsc.org/suppdata/dt/b3/b304409m/ for crystallographic data in CIF or other electronic format.

$[TlPt_6(CO)_6(PEt_3)_6][PF_6]$. M = 2396.8; monoclinic, $C2/c$, a = 22.961(2), b = 24.481(2), c = 22.451(2) Å, β = 94.795(1)°, V = 12576.0(12) $Å^3$, Z = 8; $F(000)$ = 8784; D_c = 2.532 Mg m^{-3}. 51729 reflections were obtained over $2.96 \leq 2\theta \leq 52.78°$. Empirical absorption correction (SADABS) was applied [μ(Mo-Kα) = 16.082 mm^{-1}, max./min. transmission, 0.1599/0.0565]. Full-

matrix least-squares refinement (on F^2) of 12832 independent merged reflections [R(int) = 0.0352] with 633 parameters (10 restraints on disordered carbon atoms) converged at $wR_2(F^2)$ = 0.0564 for all data; $R_1(F)$ = 0.0235 for $I > 2\sigma(I)$; max./min. residual electron density, 1.59/−1.06 e Å^{-3}. Ordered non-hydrogen atoms were refined anisotropically, while four disordered carbon atoms of two P(1)-attached ethyl groups were refined isotropically. Hydrogen atoms were included in structure factor calculations at idealized positions and were allowed to ride on attached carbon atoms with relative isotropic displacement coefficients.

$[TlPd_6(CO)_6(PEt_3)_6][PF_6]$. M = 1864.7; monoclinic, $C2/c$, a = 22.949(3), b = 24.623(3), c = 22.480(2) Å, β = 94.841(2)°, V = 12658(2) Å^3, Z = 8; F(000) = 7248; D_c = 1.957 Mg m^{-3}. 57499 reflections were obtained over $3.64 \leq 2\theta \leq 57.00°$. Empirical absorption correction (SADABS) was applied [μ(Mo-Kα) = 4.435 mm^{-1}, max./min. transmission, 0.4708/0.3496]. Full-matrix least-squares refinement (on F^2) of 15576 independent merged reflections [R(int) = 0.0329] with 631 parameters (no restraints) converged at $wR_2(F^2)$ = 0.0972 for all data; $R_1(F)$ = 0.0305 for $I > 2\sigma(I)$; max./min. residual electron density, 2.40/−0.70 e Å^{-3}. No ethyl C atoms were disordered. All non-hydrogen atoms were refined anisotropically, and hydrogen atoms were included as described above.

Acknowledgements

This research was supported by the National Science Foundation. The CCD area detector system was purchased in part in 1995 with a NSF grant (CHE-9310428). Molecular drawings were prepared with Crystal Maker, Interactive Crystallography (version 5). David C. Palmer (P.O. Box 183 Bicester, Oxfordshire, UK OXG TBS). We are grateful to Dr Ilia Guzei (UW-Madison) for crystallographic advice and thank Dr Sergei Ivanov (Los Alamos National Lab) for helpful comments.

References

1 For reviews, see: (*a*) A. D. Burrows and D. M. P. Mingos, *Coord. Chem. Rev.*, 1996, **154**, 19; (*b*) D. M. P. Mingos and R. W. M. Wardle, *Transition Met. Chem.*, 1985, **10**, 441; (*c*) R. J. Puddephatt, L. Manojlovic-Muir and K. W. Muir, *Polyhedron*, 1990, **9**, 2767; (*d*) P. Braunstein, J. Rose, in *Catalysis by Di- and Polynuclear Metal Clusters*, ed. R. D. Adams and F. A. Cotton, Wiley, New York, 1997, p. 346; (*e*) D. Imhof and L. M. Venanzi, *Chem. Soc. Rev.*, 1994, **23**, 185; (*f*) R. J. Cross, in *Comprehensive Organometallic Chemistry II*, eds.-in-chief, E. W. Abel, F. G. A. Stone and G. Wilkinson, vol. 10, ed. R. J. Puddephatt, p. 391; (*g*) P. D. Harvey, *J. Cluster Sci*, 1993, **4**, 377; (*h*) D. J. Underwood, R. Hoffmann, K. Tatsumi, A. Nakamura and Y. Yamamoto, *J. Am. Chem. Soc.*, 1985, **107**, 5968.

2 J. Chatt and P. Chini, *J. Chem. Soc. A*, 1970, 1538.

3 (*a*) J. C. Calabrese, L. F. Dahl, P. Chini, G. Longoni and S. Martinengo, *J. Am. Chem. Soc.*, 1974, **96**, 2614; (*b*) G. Longoni and P. Chini, *J. Am. Chem. Soc.*, 1976, **98**, 7225; (*c*) C. Brown, B. T. Heaton, A. D. C. Towl, P. Chini, A. Fumagalli and G. Longoni, *J. Organomet. Chem.*, 1979, **181**, 233; (*d*) L. Bengtsson-Kloo, C. M. Iapalucci, G. Longoni and S. Ulvenlund, *Inorg. Chem.*, 1998, **37**, 4335.

4 (*a*) M. F. Hallam, D. M. P. Mingos, T. Adatia and M. McPartlin, *J. Chem. Soc., Dalton Trans.*, 1988, 335; (*b*) A. Albinati, K.-H. Dahmen, A. Togni and L. M. Venanzi, *Angew. Chem., Int. Ed. Engl.*, 1985, **24**, 766; (*c*) K.-H. Dahmen, D. Imhof, L. M. Venanzi, unpublished work (mentioned in ref. 1*e*).

5 Tetrahedral μ_2-CO/PR_3-ligated (μ_3-M′)Pt_3 clusters with heterometallic M′ elements of Groups 11, 12, and 13 have also been reported.[1*a*,*c*,*e*,*f*,6] In addition, a number of related triangular triplatinum clusters with other bridging ligands (*e.g.*, SO_2, halide, and/or CNR) and other terminal donor L ligands (*e.g.*, L = CO, CNR) are known.[1*a*,*c*,*e*,*f*,6,7]

6 (*a*) C. E. Briant, R. W. M. Wardle and D. M. P. Mingos, *J. Organomet. Chem.*, 1984, **267**, C49; (*b*) P. Braunstein, S. Freyburger and O. Bars, *J. Organomet. Chem.*, 1988, **352**, C29; (*c*) S. Bhaduri, K. Sharma, P. G. Jones and C. F. Erdbrugger, *J. Organomet. Chem.*, 1987, **326**, C46; (*d*) A. Stockhammer, K.-H. Dahmen, T. Gerfin and L. M. Venanzi, *Helv. Chim. Acta*, 1991, **74**, 989; (*e*) L. Hao, L. Manojlovic-Muir, K. W. Muir, R. J. Puddephatt, G. J. Spivak, J. J. Vittal and D. Yufit, *Inorg. Chim. Acta*, 1997, **265**, 65; (*f*) O. J. Ezomo, D. M. P. Mingos and I. D. Williams, *J. Chem. Soc., Chem. Commun.*, 1987, 924; (*g*) R. Stadnichenko, B. T. Sterenberg, A. M. Bradford, M. C. Jennings and R. J. Puddephatt, *J. Chem. Soc., Dalton Trans.*, 2002, 1212.

7 (*a*) D. G. Evans, M. F. Hallam, D. M. P. Mingos and R. W. M. Wardle, *J. Chem. Soc., Dalton Trans.*, 1987, 1889; (*b*) D. Imhof, U. Burckhardt, K.-H. Dahmen, H. Rüegger, T. Gerfin and V. Gramlich, *Inorg. Chem.*, 1993, 32; (*c*) R. Ros, A. Tassan, G. Laurenczy and R. Roulet, *Inorg. Chim. Acta*, 2000, **303**, 94; (*d*) D. M. P. Mingos and R. W. M. Wardle, *J. Chem. Soc., Dalton Trans.*, 1986, 73.

8 We thank a particular referee who pointed out the fundamental problem with the *half-sandwich* description,[1*e*] which thereby led to the alternative *(open-face)-sandwich* designation presented herein.

9 (*a*) Y. Yamamoto and H. Yamazaki, *J. Chem. Soc., Dalton Trans.*, 1989, 2161; (*b*) Y. Yamamoto, H. Yamazaki and T. Sakurai, *J. Am. Chem. Soc.*, 1982, **104**, 2329.

10 (*a*) A. Albinati, A. Moor, P. S. Pregosin and L. M. Venanzi, *J. Am. Chem. Soc.*, 1982, **104**, 7672; (*b*) A. Moor, L. M. Venanzi, unpublished results mentioned in; ref. 10*a*.

11 (*a*) L. Hao, J. J. Vittal and R. J. Puddephatt, *Inorg. Chem.*, 1996, **35**, 269; (*b*) L. Hao, J. J. Vittal and R. J. Puddephatt, *Organometallics*, 1996, **15**, 3115.

12 G. J. Spivak, J. J. Vittal and R. J. Puddephatt, *Inorg. Chem*, 1998, **37**, 5474.

13 A. D. Burrows and D. M. P. Mingos, *Transition Met. Chem.*, 1993, **18**, 129.

14 (*a*) E. G. Mednikov, N. K. Eremenko, V. V. Bashilov and V. I. Sokolov, *Inorg. Chim. Acta.*, 1983, **76**, L31; (*b*) N. K. Eremenko, E. G. Mednikov, S. S. Kurasov and S. P. Gubin, *Izv. Acad. Nauk SSSR, Ser. Khim*, 1983, 682 (*Bull. Acad. Sc. USSR, Div. Chem. Sc*, 1983, **32**, 620) (Engl. Transl.); (*c*) E. G. Mednikov and N. K. Eremenko, *Izv. Acad. Nauk SSSR, Ser. Khim*, 1981, 2400 (*Bull. Acad. Sc. USSR, Div. Chem. Sci*, 1981, **30**, 1980) (Engl. Trans.)].; (*d*) E. G. Mednikov and N. K. Eremenko, *Izv. Acad. Nauk SSSR, Ser. Khim*, 1984, 2781 (*Bull. Acad. Sc. USSR, Div. Chem. Sc*, 1984, **33**, 2547) (Engl. Transl.).

15 (*a*) A. Burini, J. P. Fackler, Jr., R. Galassi, B. R. Pietroni and R. J. Staples, *Chem. Commun.*, 1998, 95; (*b*) A. Burini, R. Bravi, J. P. Fackler, Jr., R. Galassi, T. A. Grant, M. A. Omary, B. R. Pietroni and R. J. Staples, *Inorg. Chem.*, 2000, **39**, 3158; (*c*) J. P. Fackler, Jr., *Inorg. Chem.*, 2000, **41**, 6959 and references therein.

16 (*a*) J. K. Nagle, A. L. Balch and M. M. Olmstead, *J. Am. Chem. Soc.*, 1988, **110**, 319; (*b*) T. Ziegler, J. K. Nagle, J. G. Snijders and E. J. Baerends, *J. Am. Chem. Soc.*, 1989, **111**, 5631; (*c*) B. Weissbart, A. L. Balch and D. S. Tinti, *Inorg. Chem.*, 1993, **32**, 2096; (*d*) M. Dolg, P. Pyykkö and N. Runeberg, *Inorg. Chem.*, 1996, **35**, 7450; (*e*) A. L. Balch, B. J. Davis, E. Y. Fung and M. M. Olmstead, *Inorg. Chim. Acta*, 1993, **212**, 149; (*f*) K. E. Berg, J. Glaser, M. C. Read and I. Tóth, *J. Am. Chem. Soc.*, 1995, **117**, 7550; (*g*) M. Maliarik, K. Berg, J. Glaser, M. Sandström and I. Tóth, *Inorg. Chem*, 1998, **37**, 2910; (*h*) M. R. Russo and N. Kaltsoyannis, *Inorg. Chim. Acta*, 2001, **312**, 221; (*i*) J. Autschbach and T. Ziegler, *J. Am. Chem. Soc.*, 2001, **123**, 5320; (*j*) R. Usón, J. Forniés, M. Tomás and R. Garde, *J. Am. Chem. Soc.*, 1995, **117**, 1837; (*k*) R. Usón, J. Forniés, M. Tomás and R. Garde, *Inorg. Chem.*, 1997, **36**, 1383; (*l*) I. Ara, J. R. Berenguer, J. Forniés, J. Gómez, E. Lalinde and R. L. Merino, *Inorg. Chem.*, 1997, **36**, 6461.

17 V. J. Catalano, B. L. Bennett, R. L. Yson and B. C. Noll, *J. Am. Chem. Soc.*, 2000, **122**, 10056.

18 Twist angle is defined as the average angle between the following pairs of trimetal planes: M1M3M5 and M2M6M4, M1M2M6 and M3M4M5, M2M3M4 and M1M6M5 (see Fig. 1).

19 This high-nuclearity Tl_2Pd_{12} cluster, initially obtained from reactions of $Pd_{10}(CO)_{12}(PEt_3)_6$ or $Pd_4(CO)_5(PEt_3)_4$ with the phosphine-deligating $Au(SMe_2)Cl$ in the presence of the $TlPF_6$ as a chloride-scavenger, was at first formulated incorrectly as the unknown Au_2Pd_{12} cluster as a consequence of its well-determined low-temperature CCD X-ray crystal structure.[20] The wrong assignment of the two independent heavy-atom electron-density peaks as Au (Z = 79) instead of Tl (Z = 81), which would not affect the results of the least-squares refinement of the crystal structure in that X-rays are scattered by atomic electrons, arose from its molecular geometry being related to that of a previously reported Au_2Pd_{14} cluster[21] that had been prepared from an analogous reaction of $Pd_8(CO)_8(PMe_3)_7$ and $Au(PCy_3)Cl$ in the presence of $TlPF_6$. Our later realization and resulting conclusive evidence of its metal-core stoichiometry being Tl_2Pd_{12} instead of Au_2Pd_{12} was a consequence of the research

reported herein, which involved the direct preparation of the same Tl_2Pd_{12} cluster from $Pd_4(CO)_5(PEt_3)_4$ (**4**) and $TlPF_6$ (without the gold precursor); a low-temperature CCD X-ray determination gave a virtually identical solid-state structure, while $^{31}P\{^1H\}$ NMR measurements displayed analogous solution spectra (including COSY) that previously could not be satisfactorily interpreted without ^{203}Tl, ^{205}Tl coupling. Its present formulation was subsequently ascertained from an elemental analysis (Tl, Au, Pd, P).[20]

20 S. A. Ivanov, R. V. Nichiporuk, E. G. Mednikov and L. F. Dahl, *J. Chem. Soc., Dalton Trans.*, 2002, 4116.

21 R. Copely, C. M. Hill and D. M. P. Mingos, *J. Cluster Sci*, 1995, **6**, 71.

22 A. Albinati, *Inorg. Chim. Acta*, 1977, **22**, L31.

23 C. A. Tolman, *Chem. Rev.*, 1977, **77**, 313.

24 A. Moor, P. S. Pregosin and L. M. Venanzi, *Inorg. Chim. Acta*, 1981, **48**, 153.

25 This unanticipated spectral-based conclusion prompted our preparation (N. de Silva and L. F. Dahl, unpublished research, 2003) of $[(\mu_3\text{-}Tl)Pt_3(\mu_2\text{-}CO)_3(PPh_3)_3]^+$ from the corresponding reaction in THF of $TlPF_6$ with $Pt_4(\mu_2\text{-}CO)_5(PPh_3)_4$; orange–red crystals of the $[PF_6]^-$ salt of this PPh_3-ligated $(\mu_3\text{-}Tl)Pt_3$ monocation were isolated and characterized from a well-refined single-crystal X-ray diffraction determination. Its IR spectrum expectedly exhibits a single dominant carbonyl frequency at 1810 cm^{-1} in Nujol and 1818 cm^{-1} in THF. These analogous solid-state/solution single frequencies are in complete discordance with the two frequencies (*viz*., 1864(s), 1798(m) cm^{-1}, Nujol) reported[6f] for $[(\mu_3\text{-}Tl)Pt_3(\mu_2\text{-}CO)_3(PCy_3)_3]^+$ ($[PF_6]^-$ salt) but compare favorably with the single dominant frequency of 1805 cm^{-1} reported[6a] for $[(\mu_3\text{-}AuPCy_3)Pt_3(\mu_2\text{-}CO)_3(PCy_3)_3]^+$ ($[PF_6]^-$ salt). The close agreement between the dominant solid-state frequencies of 1810 and 1805 cm^{-1} for the PPh_3-ligated $(\mu_3\text{-}Tl)Pt_3$ and $(\mu_3\text{-}AuPCy_3)Pt_3$ monocations, respectively, suggests that the reduced electrophilicity of a phosphine-attached Au(I) is similar (instead of being markedly less) to that of Tl(I) in these closely related clusters. Research is currently underway to isolate and obtain single crystals of the corresponding PPh_3-attached Au(I) analogue by reaction of $[(\mu_3\text{-}Tl)Pt_3(\mu_2\text{-}CO)_3(PPh_3)_3]^+$ with $Au(PPh_3)Cl$ for structural/spectroscopic comparison.

26 Puddephatt and coworkers[12] consider the coinage d^{10} $[M']^+$ metals (M′ = Cu(I), Ag(I), Au(I)) either in sandwiches or in $[M'L]^+$ fragments (L = two-electron donor) of *open-face* sandwiches as electrophilic zero-electron donors, whereas the $5d^{10}6s^2$ Tl(I) and Hg(0) atoms are denoted as two-electron donors (which are designated as nucleophilic reagents). This formal description was then used to distinguish the varying heteroplatinum stereochemistries of their triangular-connected (*hinged*) hexaplatinum clusters in terms of different electron counts.[12] They pointed out that "although Hg(0) and Tl(I) are formally two-electron ligands, they appear to act as weakly electron-withdrawing ligands, perhaps by accepting more electron density by backbonding to empty p orbitals than they donate from the filled $6s^2$ orbitals". On the other hand, application of the PSEP model developed by Mingos[27] for high-nuclearity metal clusters would consider both the $[M'L]^+$ fragment as well as each Tl(I) and Hg(0) atom to be a 12-electron contributor to the total electron count.

27 (*a*) D. M. P. Mingos, *J. Chem. Soc., Chem. Commun.*, 1985, 1352; (*b*) D. M. P. Mingos and L. Zhenyang, *J. Chem. Soc., Dalton Trans.*, 1988, 1657.

28 S. A. Ivanov, L. F. Dahl, manuscript in preparation.

29 Noteworthy is that the closely similar Ag(I)–Pt(0) distances in the Pt_3AgPt_3 sandwich of $[(\mu_6\text{-}Ag)Pt_6(\mu_2\text{-}CO)_6(PPr^i_3)_6]^+$ (mean, 2.84 Å)[4b] are 0.1 Å longer than the Au(I)–Pt(0) distances in the Pt_3AuPt_3 sandwich of $[(\mu_6\text{-}Au)Pt_6(\mu_2\text{-}CO)_6(PPh_3)_6]^+$ (mean, 2.73 Å).[4a] The markedly shorter Au(I)–Pt(0) distances may be ascribed to the greater relativistically enhanced electrophilicity of the d^{10} Au(I). The Cu(I)–Pt(0) distances in the Pt_3CuPt_3 sandwich of $[(\mu_6\text{-}Cu)Pt_6(\mu_2\text{-}CO)_6(PPh_3)_6]^+$ (mean, 2.60 Å)[4a] are expectedly less due to the smaller Cu(I) radius.

30 J.-P. Barbier, R. Bender, P. Braunstein, J. Fischer and L. Ricard, *J. Chem. Res., (S)*, 1978, 230; J.-P. Barbier, R. Bender, P. Braunstein, J. Fischer and L. Ricard, *J. Chem. Res., (M)*, 1978, 2913.

31 (*a*) L. Pasteur, *Ann. Chim. Phys*, 1848, **24**, 442; (*b*) G. B. Kauffman and R. D. Meyers, *J. Chem. Educ*, 1975, **52**, 777.

32 (*a*) A. Moor, P. S. Pregosin, L. M. Venanzi and A. J. Welch, *Inorg. Chim. Acta*, 1984, **85**, 103; (*b*) V. F. Yudanov, N. K. Eremenko, E. G. Mednikov and S. P. Gubin, *Zh. Struct. Khim*, 1984, **25**, 49 (*J. Struct. Chem*, 1984, **25**, 41) (Engl. Transl.).

33 C. Brown, B. T. Heaton, P. Chini, A. Fumagalli and G. Longoni, *J. Chem. Soc., Chem. Commun.*, 1977, 309.

34 (*a*) R. G. Vranka, L. F. Dahl, P. Chini and J. Chatt, *J. Am. Chem. Soc.*, 1969, **91**, 1574; (*b*) R. F. Klevtsova, E. N. Yurchenko, L. A. Glinskaya, E. B. Burgina, N. K. Eremenko and V. V. Bakakin, *Zh. Struct. Khim*, 1985, **26**, 84 (*J. Struct. Chem*, 1985, **26**, 216) (Engl. Transl.).

35 Surprisingly slow rates of transformation of **2** into **5** and eventually the termination of this conversion that were observed in NMR tubes are attributed to the combination of three factors: namely, the high concentration of **2** (*viz*., ~80 mg/0.75 mL of solvent), the small area of surface between liquid and gas phase in narrow NMR tubes, and the small "free" gas volumes of these NMR tubes (~2.3 mL), which thereby maintain a relatively high residual pressure of CO *via* deligation upon conversion of **2** into **5**.

36 E. G. Mednikov and L. F. Dahl, manuscript in preparation.

37 G. Sheldrick: all crystallographic software and sources of the scattering factors are contained in the SHELXTL (version 5.1) program library, Bruker Analytical X-Ray Systems, Madison, WI.